Structural Design Airframe Variations for an

Articulated Ring-Wing eVTOL Structure with Distributed Propulsion, Advanced Dynamic Payload Stabilization, Integrated Energy Regeneration, and Safety Systems

Prepared for Aerial MECHANICA Inc.

March 29, 2026

Document Intent

This white paper defines a structural and systems-engineering framework for a family of articulated ring-wing eVTOL aircraft built from modular annulus buses carrying either 18 or 19 rotor stations per ring. The paper converts the 18-propeller UAM common-model baseline into an annular architecture that scales from a single ring to an eight-ring aircraft while preserving explicit mass, structural, electrical, and control-allocation logic. The package includes source figures, tables, code listings, equations, appendices, and a bibliography.

Contents

List of Figures

List of Tables

Abstract

This white paper defines the structural-design, sizing, and system-architecture basis for an articulated ring-wing family of distributed-electric-propulsion aircraft in which each annulus bus carries either 18 or 19 rotor stations. The central argument is architectural: a ring-wing cluster containing many small propulsors can deliver gross thrust in the class of a twin large-propeller lift aircraft while improving redundancy, actuator granularity, low-altitude controllability, and mission resilience. The paper therefore reframes the conventional radial PX4 multirotor family as a hierarchy of annulus buses. A single ring corresponds to an 18/19-rotor aircraft. Two, three, four, and eight rings scale that primitive to 36/38, 54/57, 72/76, and 144/152 rotors respectively.

The document uses the 18-propeller UAM common-model multicopter of Eze et al. [6] as the methodological foundation for mission sizing, mass closure, power estimation, electrical feasibility, and control allocation. It then extends that baseline into a ring-native structural concept in which the annulus is no longer a passive mounting frame; it becomes the primary load path, the electrical backbone, and the modular manufacturing interface. A companion Integrative Annular Conductive Chassis (IACC) concept is developed in parallel. In the IACC implementation, flat embedded power members, shielded data lanes, connector windows, and modular quick-change interconnects are packaged inside the structural ring segment rather than routed as an external harness.

The result is a technical white paper organized for engineering use. It includes the proposed rotor-coordinate function, structural sizing equations, annulus load-path definitions, wiring and power-bus architecture, control-allocation logic, budgeting, a development work-breakdown structure, test planning, appendices with code listings, and source figures. The intent is not to present an aspirational sketch. The intent is to present a directly actionable engineering package for progressing the articulated ring-wing concept from architecture definition to analytical closure, prototype build, structural substantiation, and flight-test preparation.

Executive Summary

Why the ring-wing family matters

The articulated ring-wing concept is built around a simple design choice with large downstream consequences: instead of concentrating thrust in one or two large rotors, thrust is distributed across an annular bus that is repeated as a modular airframe primitive. This choice changes the structure, the electrical distribution system, the control problem, and the fault model at the same time. The vehicle becomes more over-actuated, more redundant, and more configurable, but it also requires disciplined handling of rotor placement, current distribution, structural load sharing, and system integration.

For low-altitude operations in unstructured environments, this trade is attractive. A high-rotor annulus can soften single-point failures, reshape the control-allocation space, reduce the need for mechanically complex transmission systems, and decouple localized propulsion faults from total vehicle loss. The architecture is especially relevant when the mission values hover authority, controllable downwash, gust rejection, payload stability, and short-range operations more heavily than peak cruise efficiency. Those conditions match cargo lift, external-load movement, emergency logistics, industrial operations, and near-field passenger transport more closely than they match long-range wing-borne cruise.

Reference architecture

The reference family developed in this paper uses the following convention:

- One annulus bus: 18 or 19 rotors.
- Twin annulus: 36 or 38 rotors.
- Triple annulus: 54 or 57 rotors.
- Quad annulus: 72 or 76 rotors.
- Octo annulus: 144 or 152 rotors.

The 19-rotor form uses a center station, six inner stations, and twelve outer stations. The 18-rotor form deletes the center station and retains the 6+12 annular pattern. This geometry is not arbitrary. It is chosen because it provides a compact inner control region, a larger outer moment-arm region, and a direct mapping to bus-level segmentation.

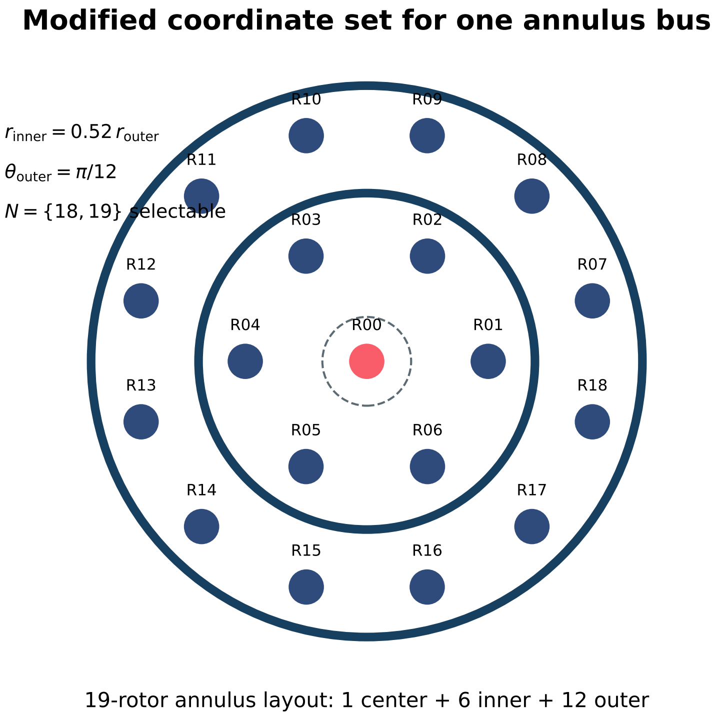

Figure 1: Normalized 19-rotor annulus layout generated for this white paper. The 18-rotor option removes the center station while preserving the inner and outer rings.

Foundation adopted from the UAM common-model work

The common-model multicopter paper provides four pieces of engineering discipline that are retained here [6]. First, it defines a mission-driven sizing loop that links TLARs, mass closure, power, mission energy, and electrical feasibility. Second, it treats control allocation as a first-class design variable rather than as an afterthought. Third, it uses explicit component roll-ups instead of opaque mass fractions wherever practical. Fourth, it exports the resulting aircraft definition as data suitable for downstream analyses.

This white paper preserves that structure and replaces the conventional radial frame with modular ring-wing buses. Every important equation is therefore asked a ring-specific question:

- How is total thrust partitioned across annulus buses?
- How does the annulus act as both the main structural member and the conductor carrier?
- Which loads are local to one ring, and which loads are shared through the core interface?
- How should the control-effectiveness matrix be layered so that each ring is both locally autonomous and globally coordinated?

Structural conclusion

The structural conclusion of this paper is that the annulus should be treated as a multi-function member with four simultaneous roles:

1. primary bending and torsion path for each ring segment,
2. mount and alignment datum for rotor, ESC, and connector hardware,
3. protected conductor package for high-current power and low-voltage data lanes, and
4. modular replacement boundary for manufacturing and field maintenance.

This is the rationale for the IACC approach. If the annulus already carries the main structural loads, then routing high-current power externally recreates avoidable harness mass, handling complexity, and packaging risk. A flat embedded conductor geometry inside the annulus reduces bundle congestion, improves manufacturability at segment interfaces, and turns the ring itself into a repeatable systems module. The repo code in the current workspace already frames the concept this way, describing "rigid flat-embedded bus bars within annular frames" and connector windows for pogo-pin or spring-finger interfaces in the system prompt logic used by the architecture app.

Programmatic conclusion

The development plan derived in this document is deliberately execution-oriented. It assumes that a full program must deliver:

- a parametric CAD and geometry-definition environment,
- ring-segment laminate and metallic insert definitions,

- an electrical architecture with deterministic parts selection,
- control-allocation logic for 18/19-per-ring deployment,
- a simulation stack covering mass, loads, power, and failure cases,
- a subscale or semi-scale build for structural and control validation, and
- a budget and work package breakdown suitable for internal planning and partner engagement.

Nomenclature

Architecture symbols

Symbol	Unit	Meaning
N_r	–	Number of rotor stations on one annulus bus (18 or 19).
N_b	–	Number of annulus buses in the aircraft.
N_t	–	Total number of rotors in the full aircraft, $N_t = N_b N_r$.
R_o	m	Outer annulus radius measured to the outer rotor ring.
R_i	m	Inner rotor ring radius. In this white paper the nominal normalized relation is $R_i = 0.52R_o$.
D_p	m	Propeller diameter.
A_d	m^2	Total actuator disk area.
m_0	kg	Maximum take-off mass.
m_{str}	kg	Structural mass.
m_{elec}	kg	Electrical distribution mass, including buses, interconnects, PDB hardware, and conductor support.
V_{bus}	V	Main DC bus voltage.
I_{bus}	A	Bus current.
B	–	Control-effectiveness matrix for the full aircraft.
u	–	Desired force/moment vector.
T	N	Rotor thrust vector.
σ	MPa	Stress.
δ	mm	Deflection.

Configuration map

Table 2: Reference annulus-bus configurations adopted throughout the document.

Configuration	Bus count N_b	Rotors per bus N_r	Total rotors N_t	PX4-style analogy
Single ring	1	18 / 19	18 / 19	single annulus lift unit
Twin ring	2	18 / 19	36 / 38	bilateral heavy-lift twin
Triple ring	3	18 / 19	54 / 57	tri-bus over-actuated frame
Quad ring	4	18 / 19	72 / 76	quadrant vehicle, PX4-style quad analogue
Octo ring	8	18 / 19	144 / 152	octagonal multi-bus aircraft

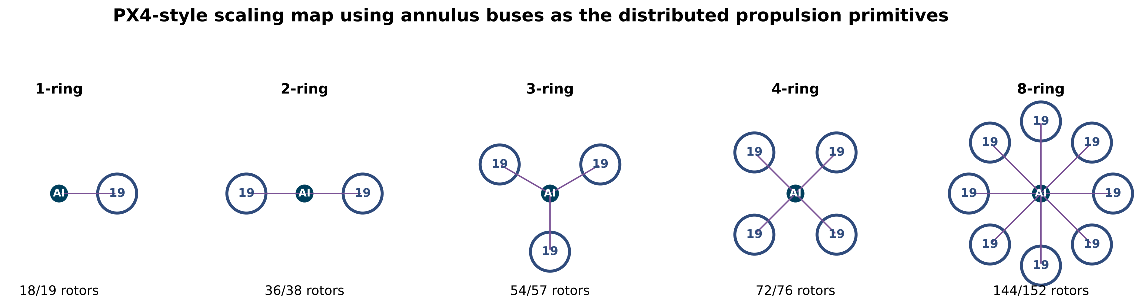

Figure 2: Scaling logic used in this white paper: annulus buses are treated as the distributed-propulsion primitives that replace conventional single-rotor arms.

Design assumptions used repeatedly

Table 3: Core assumptions used for the notional sizing and structural framing discussions. These are engineering placeholders suitable for trade studies and should be refined during concept maturation.

Item	Baseline value	Rationale
Mission type	short-range lift-centric eVTOL	Favors hover authority, redundancy, and low-altitude controllability over cruise optimization.
TLAR basis	55 km range, 100 km/h cruise, 3 occupants	Inherits the open UCM multicopter reference envelope [6].
Ring rotor count	18 or 19	Matches the app topology logic in the repository and supports center-station optionality.
Inner-to-outer radius ratio	0.52	Produces a compact 6+12 pattern with practical spacing for ring packaging.
Primary annulus material	carbon composite with metallic inserts	Balances stiffness, electrical isolation, and local fastening needs.
Embedded power backbone	flat bus bar with local shielding	Reduces harness clutter and improves modularity.
Control philosophy	hierarchical, ring-aware allocation	Each annulus is locally managed but globally coordinated by a central allocator.
Structural substantiation path	closed-form sizing → FEA → bench test → flight article correlation	Minimizes late-stage surprises in a novel frame architecture.

Chapter 1

Architecture Definition and Ring-Scaled Airframe Family

1.1 Design premise

The design premise adopted in this white paper is that an annulus bus should be treated as the equivalent of a conventional multirotor arm-plus-motor primitive, but with materially richer functionality. A traditional PX4 or ArduPilot radial multicopter places one rotor at the end of one arm. The arm is primarily structural, the wiring is external or semi-external, and the control topology treats each rotor as an individual actuator under a centralized mixer. In contrast, the articulated ring-wing concept groups 18 or 19 rotors onto a single annular frame. That annulus becomes a self-contained propulsion bus, a protected conductor carrier, and a modular replacement boundary.

This change is important because it redefines what "one corner of the aircraft" means. In a conventional quad configuration, each quadrant contains one rotor. In the annulus-bus formulation, each quadrant contains an entire ring-wing with its own local control, local structure, and local conductor package. A quad-configured aircraft therefore becomes a four-ring assembly rather than a four-motor assembly. The existing repository topology logic already captures this shift directly: if the total rotor count rises into the 72/76 range, the app maps the aircraft to a four-bus configuration, not to a 72/76-arm vehicle. That software logic aligns with the physical architecture defined here and is preserved as a design constraint.

1.2 From the UCM 18-propeller baseline to the annulus primitive

The UCM multicopter baseline is useful because it is explicit about mission sizing, mass build-up, electrical feasibility, and control allocation [6]. However, it remains a conventional radial 18-propeller frame. The present white paper converts that same system logic into a ring-native architecture as follows:

1. retain the UCM notion of an 18-propeller reference vehicle as the baseline mission-sizing problem;
2. reinterpret the 18-propeller set as a one-ring vehicle or, when a center station is added, as a 19-station annulus;
3. treat each ring as a modular bus that can be repeated around a central cabin, payload node, or core AI module;
4. carry the same force/moment control-allocation philosophy forward, but factor the control problem into ring-local and aircraft-global layers.

The consequence is that the architecture scales discretely rather than continuously. Rotor count no longer increases one motor at a time. It increases one annulus bus at a time. This is a better fit for manufacturing, replacement, logistics, and systems integration because the repeat unit is physically meaningful.

1.3 Rotor geometry and coordinate-generation rule

The annulus geometry used in this paper is driven by a modified rotor-coordinate function. The requested Mathematica pattern can be written in the following form:

Listing 1.1: Requested annulus coordinate generator for evenly spaced rotor stations on a circular path.

```
circleCoord[r_, numCircles_, thetaOffset_] :=
 Table[
   N[r*{Cos[theta + thetaOffset], Sin[theta + thetaOffset]}],
   {theta, 0, 2*Pi, (2*Pi)/numCircles}
 ][[;; -2]]
```

For the articulated ring-wing family, the generic helper above is specialized into a 19-station annulus made of one center station, six inner stations, and twelve outer stations.

The resulting logic is:

$$\mathcal{R}_{19} = \{(0,0)\} \cup \mathcal{C}(R_i, 6, 0) \cup \mathcal{C}(R_o, 12, \pi/12), \tag{1.1}$$

$$R_i = 0.52 R_o, \tag{1.2}$$

where $\mathcal{C}(r, n, \theta_0)$ denotes the evenly spaced set returned by `circleCoord`. The outer ring uses a phase shift of $\pi/12$ rad, which prevents radial alignment of every inner rotor with an outer rotor and improves packaging and wake-offset flexibility.

The 18-rotor version simply removes the center station:

$$\mathcal{R}_{18} = \mathcal{R}_{19} \setminus \{(0,0)\}. \tag{1.3}$$

The generated coordinate tables are included in the project data directory and summarized in Appendix A. They are intended for direct use in CAD, control-allocation matrix generation, and wiring-route synthesis.

1.4 Annulus bus as the aircraft primitive

The annulus bus is defined in this document as a self-contained module comprising:

- the primary ring structure, including composite skins, ribs, inserts, and rotor mounting hard-points;
- a local embedded power and data backbone;
- rotor stations, ESC or inverter interfaces, and health-monitoring nodes;
- local mounting interfaces to a center frame, cabin, or payload suspension structure; and
- local service disconnects allowing replacement of the entire ring or individual ring segments.

The distinction between bus and airframe is therefore intentionally blurred. The bus is part of the airframe, and the airframe is designed around buses rather than around isolated propulsion points. This is the structural manifestation of the patent claim family associated with the articulated ring-wing concept [7].

1.5 Family variants

1.5.1 Single-ring aircraft

A single-ring aircraft is the smallest complete expression of the architecture. It is best interpreted as a high-authority annular lifter for heavy hover, specialty cargo, or subscale validation. Its advantages are simplicity and directness: one ring, one local bus, one main conductor loop, and one global body. Its limitations are obvious as well. With only one annulus, the vehicle has fewer gross-body moment arms than the twin, triple, or quad families and therefore depends more strongly on internal thrust distribution within the ring.

1.5.2 Twin-ring aircraft

A twin-ring aircraft provides a direct comparison point against large twin-propeller or twin-rotor lift vehicles. The high-rotor substantiation summary argues that the architecture can deliver thrust in the class of a twin large-propeller eVTOL while improving redundancy and agility [1]. The annulus interpretation of that argument is more specific: instead of two dominant actuator disks, the aircraft has two large clusters of 18/19 actuators each, allowing the force command to be redistributed within each cluster before it is redistributed across the full aircraft.

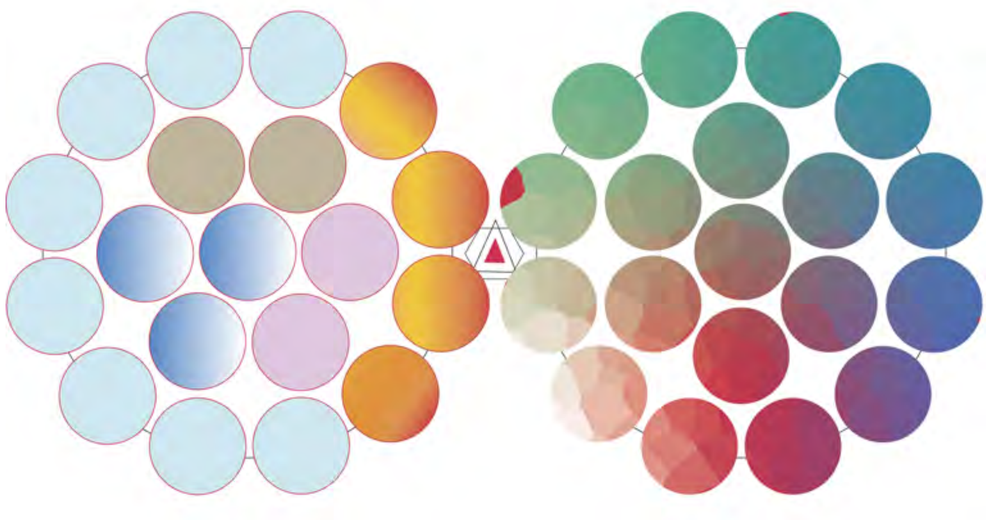

Figure 1.1: Aerial MECHANICA-provided twin-copter comparison image used as a visual reference for the twin-ring discussion.

1.5.3 Triple-ring aircraft

The triple-ring family is operationally interesting for asymmetric payloads, surveillance loiter, and dynamically biased mission loads. A three-bus architecture naturally creates one forward or upward-facing sector that can be dedicated to specialized sensor, manipulator, or payload tasks while the remaining rings maintain controllability and lift authority. The structural challenge is the central interface. Three large ring members attached to one cabin or payload core create non-trivial torsional junction loads and connector-routing density around the vehicle center.

1.5.4 Quad-ring aircraft

The quad-ring family is the most straightforward translation of the PX4 conventional quad logic into the annulus-bus world. The current repository expresses this directly: when Aerial MECHANICA selects 73–76 motors, the topology resolver returns a four-bus configuration. The 76-motor MATLAB file in the workspace provides additional evidence that the quadrant interpretation is practical. In `frameData76.m`, the 76-station system is constructed by repeating a 19-station quadrant data set four times and then enforcing symmetry in projected arm lengths, inertia, and projected area. That legacy file is not an annulus generator, but it proves that a 19-per-quadrant interpretation already exists inside the project data.

Listing 1.2: Excerpt from the workspace's 76-motor MATLAB reference showing the repeated 19-station quadrant structure.

```
motor_count = 76;
arm_lengths_quadrantA_ft = [5.4 6.7 8.1 9.8 9.0 7.8 6.2 4.6 3.5 ...
                            3.8 5.3 7.0 8.4 9.4 9.9 8.2 7.1 6.7 5.2];
arm_lengths = [arm_lengths_quadrantA_mt arm_lengths_quadrantA_mt ...
               arm_lengths_quadrantA_mt arm_lengths_quadrantA_mt];
```

In the ring-native reinterpretation proposed here, each quadrant is no longer nineteen independent arms. Each quadrant becomes one ring bus with nineteen rotor nodes embedded in a coordinated structural member. This eliminates a large amount of arm-end wiring and shifts the structural challenge from many slender cantilevers to a smaller number of stiff annular shells and their center-frame connectors.

1.5.5 Octo-ring aircraft

The eight-ring architecture is relevant when the aircraft needs extreme redundancy, sectorized payload functions, or vertiport/booster integration with symmetric loading.

It is not the most mass-efficient way to achieve a given total disk area, but it is one of the most modular. It is therefore a useful upper-end configuration for logistics, offshore service, and system-demonstrator work in which graceful degradation is valuable.

1.6 Relation to PX4-style vehicle classes

Aerial MECHANICA requested that the annular family be presented as an adaptation of the conventional PX4 radial airframe configuration. The correct interpretation is not that PX4 should remain tied to literal radial arms. Rather, the PX4 family labels become operational analogies:

- the ring is the new propulsor cluster primitive,
- the cluster occupies the positional role that one rotor previously occupied in a classical mixer,
- local rotor commands within the ring are solved by a ring allocator,
- the vehicle-level controller sees the ring as a high-authority super-actuator with internal redundancy.

This approach allows the annular aircraft to inherit familiar high-level flight-control abstractions while still using a much richer internal actuator topology.

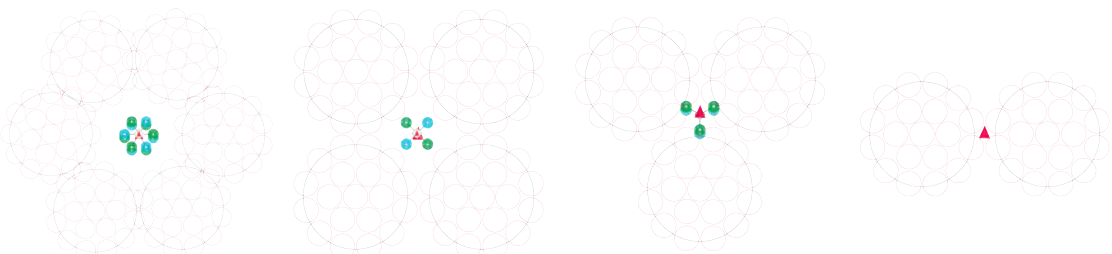

Figure 1.2: Aerial MECHANICA-provided mapping reference linking conventional radial multicopter categories to the annular-ring concept family.

1.7 Cabin, payload, and center-body integration

The core of the full-scale aircraft may be a passenger cabin, a cargo cell, an equipment bay, or a hybrid combination. The ring-wing concept remains valid across those cases because the annulus buses are attached around the core rather than through it. This creates three structural advantages:

1. the cabin can be packaged around human factors or payload needs without forcing one dominant transmission architecture through the center;
2. the annulus buses can be removed, replaced, or upgraded with reduced disturbance to the core systems; and
3. center-body structural members can be optimized for cabin and payload support rather than for carrying every rotor load directly along slender arms.

The dynamic payload-stabilization system described in the patent family further supports this center-body approach. The annulus can articulate or tune its thrust field while the cabin or payload suspension maintains a controlled attitude relative to gravity or task-specific objectives.

1.8 Architecture decisions that constrain later design work

The rest of this paper is constrained by five architecture decisions adopted here:

1. The annulus is the primary structural bus and not merely an aerodynamic shroud.
2. Rotor placement is governed by the 6+12 or 1+6+12 coordinate family.
3. Each ring is electrically segmented and serviceable.
4. Multi-ring aircraft use a hierarchical control-allocation architecture.
5. The conductor backbone is embedded and flat-packed inside the ring member.

These decisions tighten the design space on purpose. A white paper that leaves every architecture degree of freedom open is hard to execute against. A white paper that fixes the main architectural primitives can be turned into CAD, FEA, wiring, and control models without interpretive drift.

Chapter 2

Structural Design, Load Paths, and Ring Segment Sizing

2.1 Structural philosophy

The ring-wing family is structurally successful only if the annulus is allowed to do real work. A cosmetic ring that still relies on dozens of local brackets and a dense external harness defeats the purpose of the architecture. The design philosophy adopted here is therefore load-path first:

- rotor thrust enters the annulus through distributed mounting pads;
- the annulus carries local bending, torsion, and hoop response around the circumference;
- selected annulus sectors transfer resultant forces to radial struts, suspension nodes, or cabin-interface members;
- the center frame closes the global load path among rings, payload, landing loads, and inertial loads.

This philosophy yields a structure that is neither a pure conventional multicopter nor a ducted fan. It is a distributed shell-beam network made from repeating annular modules. Structural efficiency depends on matching stiffness to where the moment and interface loads actually occur rather than simply maximizing local ring thickness.

2.2 Primary structural elements

The reference full-scale airframe is decomposed into the following primary members:

1. **Annulus outer shell.** Carries the majority of local bending, distributes mount loads, and protects the embedded conductor package.

2. **Annulus inner shell or return wall.** Stabilizes the section, closes the torsion box, and creates volume for wiring or shielding layers.

3. **Ribs and webs.** Transfer point loads from motor mounts into the annulus shell while maintaining section shape.

4. **Metallic inserts and hard-points.** Carry fastener compression, bolt clamp-up, connector mounts, and high-bearing local loads.

5. **Radial struts or suspension links.** Transfer annulus resultants into the center body or articulating interface.

6. **Center-frame node.** Joins the rings to the cabin, landing gear, payload stabilization device, and any under-slung mission systems.

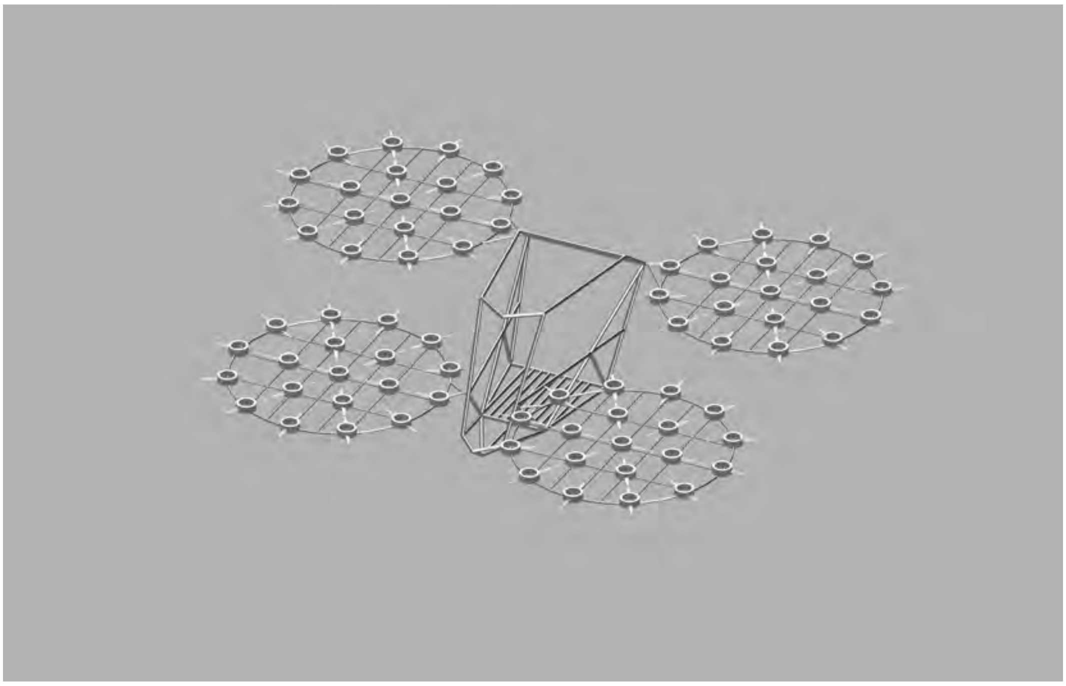

Figure 2.1: Aerial MECHANICA-provided skeletal frame reference. It is used here as a visual anchor for the idea that a multi-ring eVTOL needs explicit center-frame and cross-member definition rather than a collection of isolated rotor supports.

2.3 Load cases that govern the concept

The annulus must be sized against more than static hover thrust. The following conceptual load cases are the minimum set for early structural closure:

Table 2.1: Primary structural load cases for the articulated ring-wing family.

Case	Dominant variables	Structural significance
Hover symmetric thrust	total weight, disk loading, ring stiffness	Sets baseline annulus bending and local mount reaction loads.
Differential thrust maneuver	commanded roll/pitch/yaw moment	Identifies the worst sectors for local over-thrust and center-frame torsion.
One-rotor-out within one ring	redistribution policy, residual margin	Governs redundancy loads and local emergency authority.
One-ring degraded operation	bus isolation, neighbor-ring support	Governs central interface sizing and survivable asymmetry.
Hard landing / drop event	vertical sink rate, landing gear path	Drives center-frame crush and ring-to-core interface loads.
Gust and payload disturbance	cabin stabilization, control bandwidth	Couples structural compliance to payload motion.
Ground handling and maintenance	lifting points, segment swaps	Governs service fixtures, local dent resistance, and hard-point design.

2.4 Closed-form annulus sizing model

For early sizing, each annulus sector can be idealized as a curved beam segment between support nodes with distributed or clustered out-of-plane loads. A conservative first-order model treats the local motor load as a radial point force F_j entering a ring segment of characteristic span ℓ_s. The local bending moment scales as

$$M_j \approx \kappa_M F_j \ell_s, \tag{2.1}$$

where κ_M is a geometry factor that captures local ring continuity and support conditions. For preliminary design, κ_M may be taken between 0.20 and 0.35 depending on whether the ring is lightly or strongly coupled into a center frame.

The normal stress estimate is then

$$\sigma_{\max} \approx \frac{M_j c}{I_{\text{sec}}}, \tag{2.2}$$

where c is the outer-fiber distance and I_{sec} is the local annulus-section second moment of area. A rectangular equivalent section for the annulus wall with effective breadth b_{eff} and thickness t_{eff} gives

$$I_{\text{sec}} \approx \frac{b_{\text{eff}} t_{\text{eff}}^3}{12} \tag{2.3}$$

for local wall bending, while a closed-box annulus section should additionally be checked for torsion using

$$\tau \approx \frac{T_q}{2A_m t}, \tag{2.4}$$

where T_q is the local torque, A_m the median enclosed area, and t the effective wall thickness.

These equations are not substitutes for shell FEA, but they are useful for rapid trade studies because they show the correct architectural sensitivities: greater section depth, better closure of the annulus box, and better support spacing reduce the penalty of high rotor counts.

2.5 Material strategy

The annulus benefits from a hybrid material strategy:

- carbon or glass-carbon hybrid laminates for the main shell,
- aluminum or titanium inserts for mount-bearing areas and service interfaces,
- dielectric separators around embedded power members,
- local toughened resin or thermoplastic over-wraps where segment joints and interconnect windows are introduced.

The 2022 internal AirGo structural report is useful here because it provides a practical composite quadrant precedent. That report documented a frame assembled from three composite main rings and eight aluminum extruded tubes, with estimated total composite ring mass of roughly 2.265 kg and a quoted weight saving of approximately 77% against steel and 34% against aluminum in that specific concept [2]. The absolute numbers do not transfer directly to the present architecture, but the lesson does: ring-dominant structures become compelling when the ring itself is treated as the main composite part and metallic hardware is localized to inserts and interfaces.

2.6 Use of historical internal structural findings

Two internal structure documents inside the workspace are especially relevant for current design direction:

1. **V07 structure update.** This document described a three-ring plus tube arrangement and produced a draft structure mass estimate of about 3.45 kg for the concept as modeled [3]. Its value here is not the specific mass number; its value is the demonstration that a ring-plus-tube hybrid can be estimated systematically and reduced to interchangeable members.

2. **Composite quadrant report ARL-221111b.** This document defined composite thicknesses around 2.5 mm, modeled distributed propeller loads and counter-rotating moments, and reported a maximum displacement of 51.3 mm under the simulated condition set, with stresses stated to remain below the nominal material strength of 160 MPa [2].

Those internal results justify using a ring-dominant concept as the starting point for the current white paper rather than treating the ring as speculative geometry. They also motivate a disciplined next step: update the old composite-ring logic so it includes annulus-bus conductor cavities, segment joints, and a center-body interface appropriate for the articulated ring-wing family.

2.7 Radial struts, cabin interface, and articulation nodes

The ring itself is not sufficient. The aircraft also needs a center-body interface that can carry:

- the vector sum of ring thrust loads,
- payload and cabin inertia,
- landing and handling loads,
- actuator or articulation reaction loads, and
- local ring replacement and service loads.

When articulation is enabled, the node between annulus and center body becomes more demanding. It must allow controlled relative motion while resisting unintended play, preserving cable or bus continuity, and surviving off-design events. The safest concept at white-paper stage is a constrained interface with well-defined articulation axes, replaceable bearings or flexures, and a bounded cable or conductor transition.

2.8 Segment joints

Segment joints are unavoidable if the annulus is to be manufactured, transported, repaired, and upgraded economically. Each joint must therefore satisfy four criteria:

1. local stiffness compatible with the surrounding shell,
2. connector access for the embedded conductor package,
3. tolerance control for rotor alignment and ring circularity, and
4. maintainability under field replacement conditions.

The segment joint is also where the IACC concept becomes tangible. Instead of breaking out round wires, the joint can expose flat conductor windows and keyed shielded interfaces. This is structurally cleaner and operationally faster, provided that the inserts, clamping features, and insulation strategy are designed together rather than sequentially.

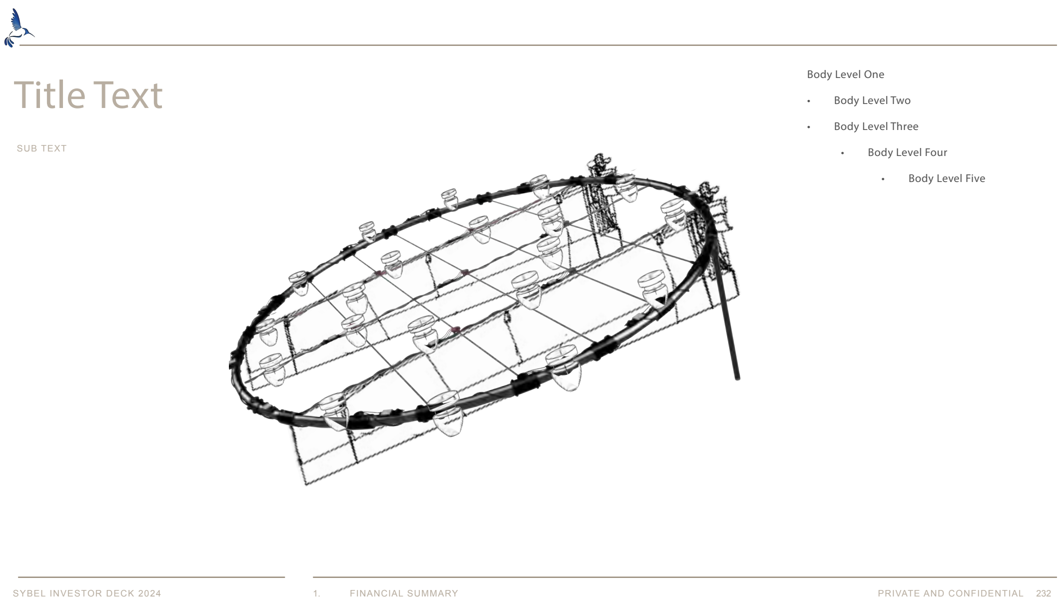

Figure 2.2: Aerial MECHANICA-provided exploded ring illustration. The image supports the modular segment discussion by showing the practicality of ring decomposition into transportable and serviceable elements.

2.9 Mass budgeting for the structure

At conceptual design stage, structural mass must be partitioned into categories that can later be correlated to CAD and FEA. A suitable breakdown is:

$$m_{\text{str}} = m_{\text{annulus}} + m_{\text{joints}} + m_{\text{radial}} + m_{\text{core}} + m_{\text{gear}} + m_{\text{payload\_support}}. \tag{2.5}$$

Each term should be estimated separately. The temptation to keep all non-propulsion mass inside one "frame fraction" is particularly dangerous in an annular aircraft because:

- conductor packaging may drive wall thickness locally,
- joint hardware adds non-trivial insert mass,
- center-body torsion can dominate even if the annulus itself is light, and
- payload stabilization hardware changes the central mass distribution.

2.10 Deflection targets

The ring-wing family should be designed to explicit compliance targets rather than simply to stress allowables. Excess compliance hurts:

- rotor-tip clearance control,
- control-effectiveness predictability,
- passenger and payload stability,
- bus-interconnect durability, and
- acoustic repeatability.

For initial work, a practical target is to keep worst-case static annulus-tip displacement below roughly 2–3% of local rotor diameter under the limit hover-plus-maneuver load case, with tighter targets for segment-joint mismatch and rotor-mount differential motion. The old internal report's 51.3 mm deflection result is useful as a reference order of magnitude, not as a design limit, because the present architecture changes ring depth, conductor routing, and support conditions.

2.11 Structural verification sequence

The recommended verification sequence is:

1. compute closed-form annulus sizing for wall thickness, section depth, and support spacing;
2. generate CAD with explicit inserts, conductor cavities, and segment joints;
3. run shell or solid FEA for the minimum load cases in Table 2.1;
4. build a representative ring segment or ring quadrant for stiffness and joint testing;
5. correlate FEA to measured deflection and strain;
6. freeze the structural template before major electrical and flight-test integration.

This sequence is deliberately strict. Structural novelty compounds quickly when the airframe, wiring, and modular service concept are all changed simultaneously. The cost of disciplined correlation early is lower than the cost of discovering that a conductor cavity or joint window has become the dominant structural weakness after flight hardware is built.

Chapter 3

Sizing Methodology, Power, Energy, and Structural Analysis Workflow

3.1 Mission-driven sizing loop

The sizing loop in this white paper inherits the UCM multicopter discipline: mission assumptions, mass closure, power requirement, energy requirement, electrical feasibility, and component selection must be solved together rather than as isolated calculations [6]. The annulus-bus architecture adds a further requirement: the structural member that carries the propulsion loads is also the member that carries the conductor system. For that reason, the sizing loop in Figure 3.1 should be understood as a multi-domain loop, not a purely aerodynamic or mass-estimation loop.

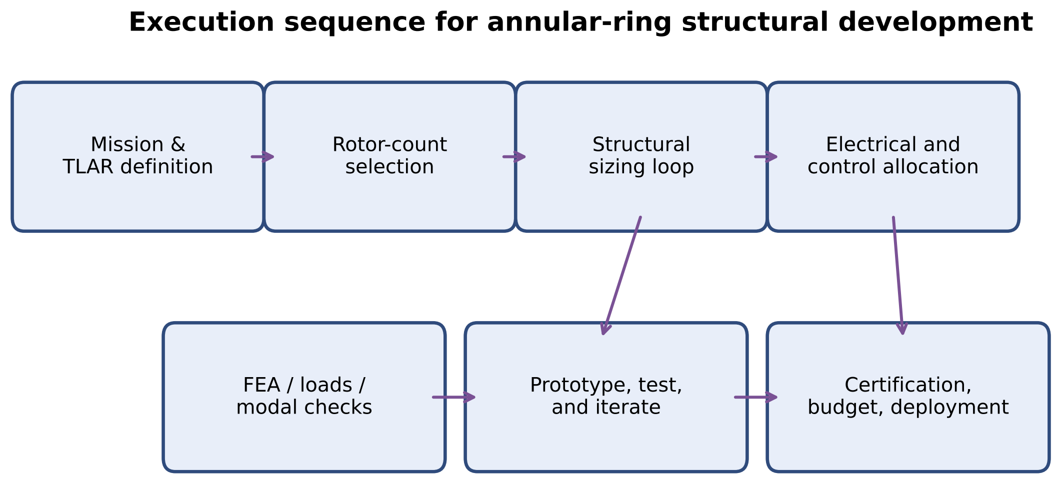

Figure 3.1: Engineering workflow used in this white paper. Mission definition, rotor-count selection, structural sizing, electrical architecture, and verification are coupled rather than sequentially isolated.

3.2 Mass closure

The first useful sizing relation remains the maximum-takeoff-mass closure:

$$m_0 = m_{\text{payload}} + m_{\text{bat}} + m_{\text{str}} + m_{\text{prop}} + m_{\text{elec}} + m_{\text{av}} + m_{\text{misc}}. \tag{3.1}$$

What changes in the annular architecture is the interpretation of m_{str} and m_{elec}. In a conventional aircraft these may be loosely separable. Here they are partly co-designed because conductor cavities, joint windows, shielding layers, and annulus hard-points alter both structural thickness and electrical mass. The correct engineering approach is therefore to preserve separate mass buckets while allowing them to influence one another in the iteration.

For battery-electric missions,

$$m_{\text{bat}} = \frac{E_{\text{req}}}{e_{\text{pack}}}, \tag{3.2}$$

where E_{req} is the mission energy including reserve and e_{pack} is the pack-level specific energy including structural packaging, thermal management, safety electronics, and mechanical containment.

3.3 Thrust and disk area

For an aircraft of mass m_0 in hover,

$$T_{\text{tot}} \approx m_0 g, \tag{3.3}$$

and the average per-rotor thrust for an N_t-rotor aircraft is

$$T_r = \frac{m_0 g}{N_t}. \tag{3.4}$$

This simple equation is one of the key benefits of high rotor count: for fixed total weight, the average thrust per rotor drops as the number of active stations rises. That reduction does not magically remove structural requirements, but it does lower the per-station load entering each local mount. For the annular architecture this is particularly useful because it allows the ring wall to be sized around many smaller inputs rather than a few very large ones.

Total disk area is

$$A_d = N_t \frac{\pi D_p^2}{4}. \tag{3.5}$$

The disk-loading trade is then

$$\text{DL} = \frac{m_0 g}{A_d}. \tag{3.6}$$

Larger propellers reduce induced power but may expand annulus diameter, reduce packaging margin, increase overlap risk, and increase ring bending leverage. Therefore the best annular design point is not found by maximizing rotor diameter alone.

3.4 Hover power and ring-level implications

Using actuator-disk reasoning, the induced hover power scales as

$$P_{\text{ind}} \approx \frac{T_{\text{tot}}^{3/2}}{\sqrt{2\rho A_d}\, FM}, \tag{3.7}$$

where FM is a hover figure of merit. The value of this equation for structure is indirect but important: higher hover power drives higher conductor current, larger wire or bus cross-sections, higher thermal loads in enclosed cavities, and larger battery mass. In the annulus-bus concept, these electrical consequences feed back into structural thickness and joint design.

3.5 Adapting the UCM worked example

The UCM multicopter paper reported a corrected worked example with approximate values of

- $m_0 \approx 1210\,\mathrm{kg}$,
- $m_{\mathrm{bat}} \approx 525\,\mathrm{kg}$,
- total disk area $\approx 74.8\,\mathrm{m}^2$,
- disk loading $\approx 159\,\mathrm{N/m}^2$,
- induced hover power $\approx 128\,\mathrm{kW}$, and
- mission energy requirement $\approx 121\,\mathrm{kWh}$,

for the 18-propeller common-model baseline [6]. This white paper does not claim those exact values for every annulus family member. Instead, it uses them as a foundational order-of-magnitude check.

The interpretation for the one-ring 18/19-rotor vehicle is straightforward: the UCM 18-propeller vehicle can be re-expressed as an annulus with similar total rotor count but different local geometry and structural packaging. For the quad-ring 72/76-rotor family, the same mission class can be attacked two different ways:

1. maintain similar gross weight while lowering per-rotor loading and increasing redundancy, or
2. scale gross weight upward while preserving per-rotor thrust and motor selection bands.

This is one reason the ring family is powerful analytically. Adding rings does not only add thrust. It changes the feasible combinations of disk loading, redundancy, motor selection, and structural segmentation.

3.6 Electrical feasibility and deterministic parts selection

The UCM methodology insists that electrical feasibility be checked explicitly [6]. The referenced repository by Minpei Chua provides a useful practical analogue because it stores deterministic CSV databases for motors, batteries, PDBs, and wire-routing outputs [4]. After cloning the repository during this task, the following schema was confirmed:

- motor database entries with weight, nominal voltage, max current, and max thrust;
- battery database entries with weight, nominal voltage, discharge current, and capacity;
- PDB entries with weight, max number of inputs, and current limit;
- structural frame data with motor positions and geometric metadata; and
- wire-routing outputs giving required conductor lengths and capacitor requirements for a 32-motor example.

This structure is directly reusable. An annulus-bus version should preserve the deterministic pattern while expanding the database to ring-specific components such as segment interconnects, bus-bar laminates, local isolation modules, and annulus service joints.

Table 3.1: Example schema confirmed from the external parts-selection repository cloned for this task.

File family	Example fields	Relevance to the annulus family
Motor CSV	weight, nominal voltage, max current, max thrust	Supports per-station thrust margin and mass roll-up.
Battery CSV	weight, nominal voltage, discharge current, capacity	Supports bus voltage selection and reserve analysis.
PDB CSV	weight, max inputs, max current	Supports segmented annulus power distribution design.
Position CSV	motor number, x, y, spin direction	Supports control-allocation and wiring-route generation.
Wire requirements text	conductor lengths by gauge and function	Supports conductor mass and packaging estimates.

3.7 Wire-length and conductor-mass implications

The external repository's 32-motor example reported, for one configuration, approximately 63 m each of positive and negative 16 AWG wire from fuselage to ESCs, 3 m per phase from ESCs to motors, and roughly 23 m each of CAN ground, CAN-L, and CAN-H wire. Those results are useful because they quantify what happens in a conventional routed system: as motor count grows, wiring becomes a mass, routing, and maintainability issue in its own right.

The IACC concept addresses exactly this problem by embedding the dominant power lanes inside the ring member. A ring-local conductor package does not eliminate wiring, but it relocates it into a repeatable structural cross-section. That significantly improves routing determinism and reduces ad hoc bundle accumulation at the vehicle center.

Conductor mass can be estimated as

$$m_{\text{cond}} = \sum_k \rho_k A_k L_k, \tag{3.8}$$

where each conductor family k has density ρ_k, cross-sectional area A_k, and total routed length L_k. In the annulus case, L_k is driven much more by segment length and ring count than by arbitrary harness routing. That is a key architectural simplification.

3.8 Structural sizing loop with embedded electrical penalties

Because the annulus contains both structure and conductors, the sizing loop should be executed in the following order:

1. choose rotor count per ring, propeller diameter, and target gross weight;
2. estimate ring diameter and support spacing;
3. compute thrust, hover power, and initial bus current;
4. size the conductor package required by current and thermal limits;
5. update annulus wall thickness, inserts, and joint geometry to accommodate the conductor package;
6. recompute structural mass and total aircraft mass;
7. iterate until both mechanical and electrical margins are satisfied.

This order matters. If the conductor package is added after the structural geometry is fixed, the annulus section will often become either too thin locally or too bulky globally. If it is included early, the ring can be sized once rather than repeatedly patched.

3.9 Modal and stiffness analysis

High rotor counts do not remove the need for modal analysis. In fact, they intensify it because the propulsion system can excite many spatial harmonics around the ring. The minimum structural analysis set should therefore include:

- first six global modes of the complete vehicle,
- first several local annulus shell modes,
- segment-joint flexibility sensitivity,
- motor-mount local modes,
- cabin or payload suspension modes, and
- coupled modes involving radial struts and annulus bending.

The 2022 internal composite report already performed an early modal check on a related ring-dominant concept [2]. The present white paper extends that logic by emphasizing that mode placement is not only a structure problem; it also determines how safely the high-rotor control allocator can command rapid differential-thrust maneuvers.

3.10 Control-effectiveness matrix generation from geometry

For a full N_t-rotor aircraft, the control-effectiveness matrix depends on each rotor position vector r_j, thrust axis n_j, and spin-dependent reaction coefficient. The ring-coordinate function introduced earlier is therefore not merely a plotting tool. It is the generator for the actual control geometry. Once a ring's rotor set is known, the aircraft-level effectiveness matrix can be built by translating and rotating that ring into each bus position around the center frame.

This is analytically cleaner than manually defining each actuator position because it preserves exact symmetry and makes degradation studies easier. If one ring is removed or isolated, the same generator can rebuild the reduced aircraft matrix with a known geometry rather than a hand-edited one.

3.11 Practical output set for the sizing workflow

Every sizing run should emit more than total mass. The minimum useful output set is:

- total mass and mass breakdown by structure, propulsion, electrical, avionics, payload, and reserve,
- total and per-rotor thrust,

- disk area and disk loading,
- hover, climb, cruise, and reserve power,
- bus voltage, bus current, and ring-local current,
- annulus section size, segment count, and joint count,
- conductor lengths and conductor mass by function,
- center-frame reaction loads by flight condition,
- first-order natural frequencies, and
- allocator feasibility under representative failure cases.

If any of these are missing, the result is difficult to pass downstream into CAD, FEA, or controls. The white paper is written to avoid that failure mode.

Chapter 4

IACC Electrical Backbone, Control Allocation, Safety, and Operations

4.1 Integrative Annular Conductive Chassis concept

The Integrative Annular Conductive Chassis (IACC) is the systems-engineering counterpart to the annulus structural concept. It starts from a negative observation: conventional multirotor electrical architecture scales poorly when every new actuator adds new harness congestion, new routing exceptions, and new service labor. In a 72/76-rotor or 144/152-rotor aircraft this becomes a dominant integration problem.

The IACC response is to package the dominant power and data paths inside the ring member itself. The annulus is therefore not only a mechanical shell but also a conductor carrier. In practical terms, each ring segment contains:

- one or more flat embedded power members sized for local current sharing,
- parallel low-voltage or differential data lanes,
- shielding and isolation layers separating high-current and low-level signals,
- connector windows at segment boundaries, and
- local breakout features only where ESCs, inverters, or sensors actually need access.

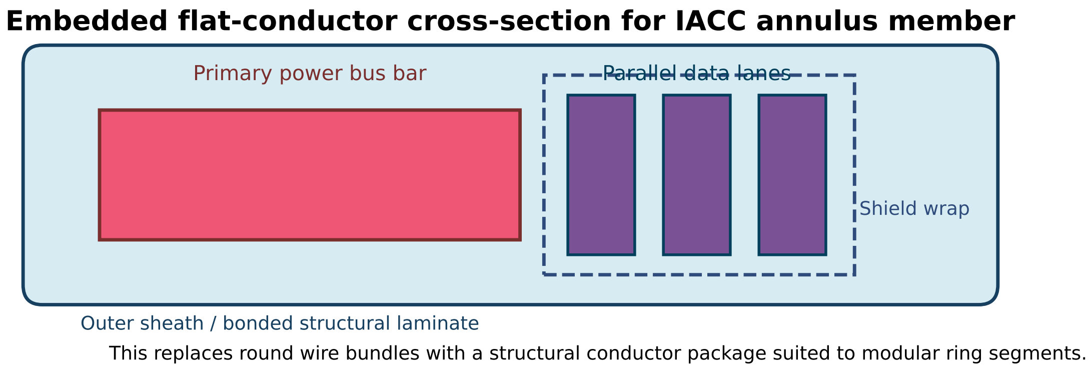

Figure 4.1: Conceptual cross-section for an embedded conductor package inside an annulus member. The power bus bar is broad and flat, while data lanes are grouped and shielded separately inside the same structural package.

4.2 Why flat embedded geometry is preferable to round bundles

Aerial MECHANICA specifically requested a shift from round wire bundles to a flat embedded geometry with a central bus bar for power and parallel conductors for data. This request is sound for four engineering reasons:

1. **Packaging efficiency.** Flat conductors use radial depth more effectively inside a thin annulus wall and simplify shield placement.
2. **Repeatability.** Once the annulus section is defined, conductor location becomes deterministic rather than a routing afterthought.
3. **Modularity.** Segment joints can expose wide, keyed conductor windows rather than loose wire pigtails.
4. **Serviceability.** Local damage and replacement are easier to isolate when the ring is partitioned into repeatable conductor-bearing segments.

This is also consistent with the current repository's IACC patent-drafting logic, which explicitly describes "rigid flat-embedded bus bars within annular frames" together with connector windows and shielded data channels. The white paper adopts that concept as a concrete engineering baseline rather than as a generic aspiration.

4.3 Interconnect strategy

The interconnect system is the enabling detail that turns IACC into a modular assembly method. A useful segment-interface concept includes:

- a structural tongue-and-groove or scarf geometry for shell alignment,
- metallic inserts or floating nuts for clamp-up,
- a recessed electrical window exposing plated bus surfaces or mating pads,
- spring-finger or pogo-style contact elements mounted in a protected cartridge, and
- an environmental seal that closes after structural fasteners are installed.

The sequence should be intentionally simple: align the segment, mechanically clamp it, engage the contact cartridge, and verify continuity through automated ring-health diagnostics. This is far more scalable than manually terminating dozens of separate conductors in each maintenance event.

4.4 Bus segmentation and fault containment

Each ring should be electrically segmented into zones. Segmenting the ring serves three purposes:

1. it limits fault propagation from a local short or thermal event,
2. it allows local isolation for maintenance or degraded operation, and
3. it preserves part of the ring's functionality even if one segment must be taken offline.

For example, a 19-station ring may be partitioned into four or six electrical sectors even though it remains one mechanical ring. Sectoring the bus is especially important when the aircraft uses decentralized battery modules or zone-local PDB hardware, as proposed in the patent family [7].

4.5 Battery architecture and local energy safety

The articulated ring-wing concept explicitly benefits from decentralized battery modules rather than from one monolithic pack. The safety case is stronger when the aircraft uses several independently monitored modules because thermal, electrical, and mechanical faults can be localized. This is aligned with the patent language describing decentralized battery modules and anti-runaway disconnect behavior [7]. It also aligns with EASA's explicit concern for battery thermal-runaway design and installation [5].

Figure 4.2: Aerial MECHANICA-provided battery module image used as a reference for the decentralized energy-module discussion.

The battery architecture recommended here has three layers:

- **Vehicle layer.** Overall bus-voltage selection, reserve policy, and central energy-management logic.
- **Ring layer.** Ring-local current monitoring, fault isolation, and health reporting.
- **Module layer.** Cell protection, thermal sensing, local disconnects, and runaway containment.

4.6 Energy regeneration

Integrated energy regeneration is meaningful only when it is attached to an explicit system boundary. In this white paper, regeneration is considered in three places:

1. **Descent and transient electrical recovery.** Limited recovery through motor-inverter control during suitable operating conditions.
2. **Ground infrastructure interaction.** Vertipad or booster modules that capture useful flow energy near landing or stationary operations.
3. **Mission ecosystem integration.** Shared energy modules or field systems that reduce dependence on one centralized charging architecture.

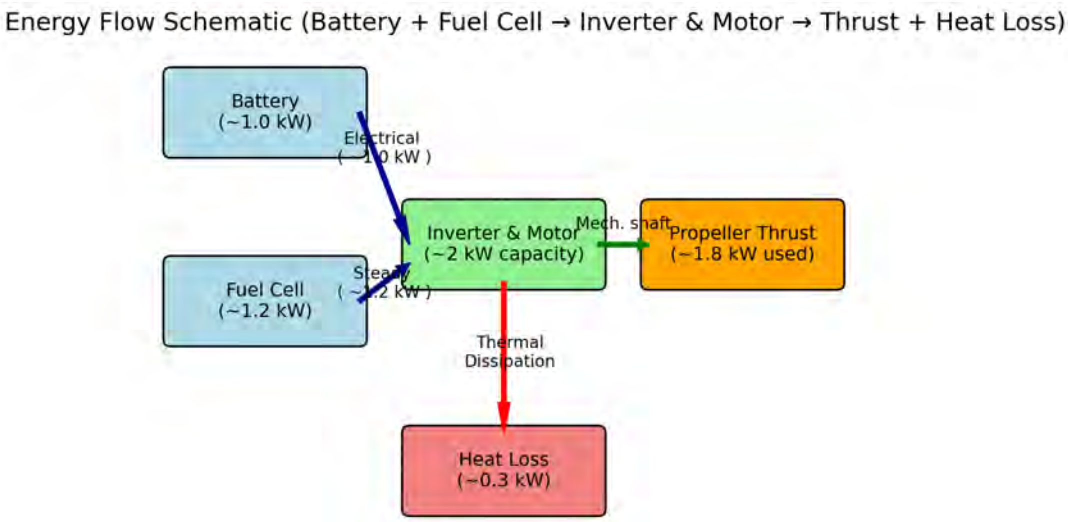

Figure 4.3: Aerial MECHANICA-provided energy-flow schematic used as a qualitative reference for the integrated regeneration discussion.

The practical engineering stance is conservative: regeneration is treated as margin improvement and ecosystem leverage, not as the primary energy source for mission closure. Structural and powertrain sizing should therefore remain valid even if regeneration contributes only a modest fraction of the total energy budget.

4.7 Control allocation hierarchy

The UCM baseline already states the over-actuated control-allocation problem clearly: for $N_r > 4$, the aircraft has more independent thrust actuators than controlled rigid-body degrees of freedom [6]. The annulus family intensifies that property and suggests a hierarchical allocator.

The proposed hierarchy is:

1. **Vehicle allocator.** Solves the global force/moment demand for the whole aircraft and distributes equivalent commands to the annulus buses.
2. **Ring allocator.** Converts each bus command into individual rotor thrust targets within that ring while respecting local limits and health status.
3. **Motor controller layer.** Tracks commanded rotor thrust or speed, manages local current and thermal limits, and reports health state upstream.

At the full-aircraft level, the unconstrained minimum-norm allocation remains

$$T^{\star} = B^{\dagger}u, \tag{4.1}$$

where B is the aircraft control-effectiveness matrix and u is the demanded force/moment vector. In practice the constrained problem is more useful:

$$\min_{T} \|W(T - T_0)\|_2^2 \quad \text{subject to} \quad BT = u,\ T_{\min} \leq T \leq T_{\max}, \tag{4.2}$$

with W chosen to reflect efficiency, thermal margin, noise management, or structural load relief priorities.

4.8 Ring-aware allocation and structural load relief

One of the strongest arguments for a high-rotor annular architecture is that control-allocation degrees of freedom can be used for more than rigid-body tracking. In this document, the allocator is assumed to have secondary objectives such as:

- minimizing peak thrust in the most highly stressed annulus sectors,
- limiting current spikes in one power segment,
- avoiding repeated excitation of one structural mode,
- keeping one sector cool after a thermal transient, and
- redistributing load away from a damaged or degraded segment.

This is where structure and controls genuinely merge. A novel airframe should not wait for structural constraints to be violated before the controller reacts. It should allocate thrust so that structural extremes are avoided during normal operation whenever excess authority is available.

4.9 Failure cases

The architecture should explicitly support the following failure cases:

- single rotor failure inside one ring,
- ESC or inverter failure,
- one local bus segment isolated,
- one decentralized battery module disconnected,
- one annulus bus degraded but not fully removed,

- central data-lane interruption with ring-local continuation, and
- articulation lockout or payload-stabilization reversion.

The key design rule is that not every failure should require immediate vehicle abandonment. The architecture is valuable precisely because it has multiple independent thrust channels, multiple local energy zones, and local segment isolation potential.

4.10 Noise and operational profile

The high-rotor substantiation summary frames the noise argument qualitatively: many smaller blades shift acoustic content toward higher frequencies and may create a softer community noise signature than a twin large-propeller system [1]. The correct engineering interpretation is cautious. High rotor counts do not guarantee low noise; they create a different noise design space. Rotor phasing, spacing, loading, structural compliance, and control scheduling all matter.

The allocator should therefore be allowed to carry noise-aware objectives. For example, if the aircraft has excess lift authority during approach, it may deliberately avoid synchronized operating points that maximize tonal reinforcement between neighboring sectors. This idea is consistent with existing UAM noise-framework research [8].

4.11 Dynamic payload stabilization

Dynamic payload stabilization is structurally relevant because it changes how the center body is used. In a conventional heavy-lift multicopter, the flight controller often fights disturbance through whole-body thrust changes alone. In the articulated ring-wing family, two layers are available:

1. the aircraft can redistribute thrust globally and locally across rings; and
2. the payload or cabin support can be isolated or actively stabilized relative to the ring frame.

This can reduce transient payload excursions and, when designed correctly, reduce structural shock loading into the central frame during gusts or abrupt maneuvers. It also creates a clearer human-factors path for passenger variants because the cabin can be protected from some fraction of the ring motion and downwash-driven disturbance.

4.12 Implications for software and avionics

The avionics stack should be designed around bus awareness, not just around actuator count. At minimum, each annulus bus should report:

- segment voltages and currents,
- local temperatures and connector health,
- rotor availability and performance margin,
- articulation or joint state where relevant, and
- local estimator confidence and communications quality.

The core AI or flight computer then reasons at the bus level first and the rotor level second. This is computationally cleaner and operationally more informative than flattening a 76- or 152-rotor aircraft into one undifferentiated actuator list.

Chapter 5

Tooling, Task Execution Plan, Verification Roadmap, and Budget

5.1 Execution principle

The execution plan in this chapter is written for engineering action rather than for concept promotion. The objective is to turn the articulated ring-wing family into a substantiated structural and systems design package that can support detailed design, prototype release, and disciplined test activity. That requires more than a CAD model. It requires a reproducible chain linking geometry generation, structural analysis, electrical architecture, parts selection, control allocation, manufacturing definition, and test correlation.

5.2 Recommended toolchain

Table 5.1: Recommended toolchain for the next phase of ring-wing development. Equivalent tools may be substituted as long as input and output interfaces remain stable.

Domain	Preferred tooling	Output needed
Parametric geometry	CAD with scriptable parameters plus exported CSV coordinates	ring diameters, segment geometry, joint positions, mount references
Structural analysis	shell/solid FEA with modal and static cases	stress, strain, displacement, buckling, mode shapes
Rotor layout	Mathematica, MATLAB, or Python generator tied to CAD export	rotor coordinates, ring transforms, control-effectiveness input
Mass and power sizing	MATLAB or Python notebooks derived from UCM logic	mass closure, power, energy, voltage/current, reserve sensitivity
Parts selection	deterministic CSV-backed scripts	selected motors, packs, PDBs, conductor lengths, interconnect bill of materials
Control allocation	MATLAB/Python simulation and flight-control implementation	B matrix, constrained allocation, failure-mode response
Electrical design	schematic capture plus harness/bus-bar definition	ring segmentation, interconnect windows, isolation logic
Test data	synchronized logging and post-processing stack	structural correlation, current, temperature, thrust, and flight-state data

5.3 Step-by-step execution plan

5.3.1 Phase 1: architecture freeze

The first phase establishes the shape of the product family before expensive detail work begins.

1. Freeze the ring-count family map: single, twin, triple, quad, and octo.
2. Freeze the rotor-station pattern: 18 or 19 per annulus using the 6+12 or 1+6+12 layout.

3. Select the initial design point for detailed closure. The recommended starting point is the quad-ring 72/76 family because it directly matches the quadrant interpretation already present in the workspace code and MATLAB references.
4. Freeze the center-body strategy: passenger cabin, cargo cell, or test article.
5. Freeze the annulus segmentation strategy and joint count.

5.3.2 Phase 2: parametric geometry and ring interfaces

1. Generate the ring-coordinate tables and import them into CAD.
2. Build parametric annulus geometry with adjustable wall thickness, insert sizes, and conductor cavities.
3. Define radial struts, cabin interfaces, articulation axes, and landing-load paths.
4. Export geometry attributes to structural and control models.

5.3.3 Phase 3: mass, power, and conductor closure

1. Adapt the UCM mass and power loop to the chosen ring-count configuration.
2. Expand the deterministic component-selection database to annulus-specific hardware.
3. Calculate current per ring, per segment, and at the center-body interface.
4. Size flat bus members, shielding layers, and segment interconnect windows.
5. Update structural mass to include the embedded conductor package.

5.3.4 Phase 4: structural analyses

1. Run annulus-only static and modal FEA.
2. Run full-ring plus center-body static cases.
3. Run one-rotor-out and one-segment-isolated differential load cases.
4. Correlate section depth, insert size, and joint geometry to displacement and stress limits.
5. Freeze a representative ring segment and a representative full annulus for prototype manufacture.

5.3.5 Phase 5: controls and avionics integration

1. Generate the aircraft-level control-effectiveness matrix from rotor coordinates.
2. Implement the ring-aware hierarchical allocator.
3. Add structural load-relief weighting and thermal/current constraints.
4. Validate degraded-mode controllability under rotor, segment, and battery-module outages.
5. Define telemetry and health messages at the ring and segment levels.

5.3.6 Phase 6: prototype and test

1. Manufacture ring coupons and segment joints for mechanical testing.
2. Manufacture a representative powered ring for current, temperature, and stiffness testing.
3. Manufacture a center-body interface rig for static and dynamic loading.
4. Build a semi-scale or heavy subscale integrated article.
5. Correlate test data to the analytical models and update the design freeze.

5.4 Verification matrix

Table 5.2: Recommended verification matrix from concept through integrated prototype testing.

Verification item	Method	Exit criterion
Rotor coordinate generator	analytical / software test	deterministic coordinates for all family variants
Mass and power loop	notebook regression	repeatable closure within tolerance and documented assumptions
Bus-bar sizing	thermal-electrical calculation	current density, temperature rise, and insulation margins met
Segment joint stiffness	coupon and subassembly test	measured stiffness within correlation band to FEA
Annulus displacement	static test and FEA	worst-case displacement within design target
Modal placement	modal test and FEA	first critical modes separated from dominant operating excitations
One-rotor-out handling	simulation and bench HIL	controlled response with bounded thermal/current margin
Ring isolation behavior	hardware and software test	no unsafe fault propagation across ring sectors
Battery isolation and safety	electrical test	controlled disconnect and protected fault handling
Integrated prototype performance	tethered and free-flight test	force authority, thermal margins, and controllability confirmed

5.5 Work breakdown structure

Table 5.3: Suggested work breakdown structure for the next major engineering phase.

WBS	Work package	Duration	Main deliverables
1.0	Program systems engineering	18 months	requirements, interfaces, design reviews, configuration control
1.1	Architecture baseline freeze	2 months	ring-count selection, coordinate family, center-body concept
1.2	Interface management	18 months	CAD/analysis/control data exchange definitions

WBS	Work package	Duration	Main deliverables
2.0	Parametric geometry and CAD	4 months	annulus templates, joints, inserts, center-body CAD
2.1	Rotor coordinate integration	1 month	CAD-driven rotor placement and export
2.2	Annulus segmentation design	2 months	segment boundaries, joint concepts, service access
3.0	Structural analysis	5 months	static, modal, joint, and degraded-case FEA reports
3.1	Coupon and joint test articles	3 months	test fixtures, stiffness and failure correlation
3.2	Ring test article	2 months	powered annulus bench article
4.0	Electrical architecture and IACC	5 months	bus-bar sections, interconnects, ring segmentation, protection logic
4.1	Deterministic parts database expansion	2 months	motors, modules, inverters, interconnect BOMs
4.2	Conductor thermal validation	2 months	current and temperature validation campaign
5.0	Controls, simulation, and avionics	5 months	hierarchical allocator, HIL setup, health reporting
5.1	Failure-mode simulation	2 months	one-rotor-out, one-segment-out, one-ring-degraded results
5.2	Noise-aware allocation logic	2 months	phased-command scheduler and assessment logic
6.0	Prototype integration and test	6 months	semi-scale or heavy-subscale demonstrator, tethered test, flight test
6.1	Ground verification	2 months	structural bench, current, thermal, and power tests
6.2	Flight envelope expansion	3 months	progressive hover and maneuver envelope build-up
7.0	Safety and certification pathfinding	4 months	failure assessment, reserve logic, compliance matrix, test evidence map

5.6 Budget basis

The budget below is a notional engineering-program estimate for one serious concept-maturation cycle. It assumes a small but competent multidisciplinary team, limited outsourced fabrication, and a semi-scale or heavy-subscale prototype campaign before any full-scale article. It is not a production budget and not a certification budget. It is the budget required to credibly establish the architecture.

Table 5.4: Illustrative budget for a 15–18 month annular ring-wing concept maturation program.

Cost element	Estimate [USD]	Notes
Lead structures engineer and analyst effort	240,000	FEA, loads, joints, structural closure
Electrical architecture and power systems effort	180,000	IACC, modules, isolation, conductor thermal design
Controls and avionics effort	180,000	allocator, fault logic, integration, HIL
CAD and design engineering support	140,000	annulus templates, interfaces, manufacturing definition
Prototype fabrication and tooling	260,000	molds, inserts, fixtures, machined joints, powered rings
Battery, inverter, motor, and power hardware	180,000	development hardware, spares, instrumentation
Test equipment and instrumentation	95,000	DAQ, strain, thermal, current, thrust, safety equipment
Ground and flight test operations	160,000	site access, support equipment, operators, logistics
Software, compute, and data infrastructure	60,000	simulation, storage, analysis environment, HPC or cloud time
Safety reviews, compliance consulting, and documentation	75,000	compliance matrix, hazard analysis, review packages
Contingency (15%)	235,500	recommended for novel architecture risk
Total	1,805,500	concept maturation through integrated prototype evidence

5.7 Staffing model

The minimum useful team for this phase is:

- one lead systems architect,
- one lead structural engineer,
- one electrical/power systems engineer,
- one controls and flight software engineer,
- one CAD/manufacturing engineer,
- one test and integration lead, and
- part-time specialist support in certification, acoustics, and materials.

Trying to compress this work into only controls or only CAD effort will fail because the airframe novelty is cross-domain by definition.

5.8 Decision gates

The program should pass through at least four explicit gates:

1. **Gate A: architecture gate.** Ring count, geometry family, and IACC section approved.
2. **Gate B: substantiation gate.** Static, modal, and conductor analyses correlated to coupon or segment tests.
3. **Gate C: integration gate.** Ring allocator, power segmentation, and health reporting demonstrated on hardware.
4. **Gate D: flight gate.** Integrated prototype cleared for progressive tethered and then untethered testing.

5.9 Major risks and mitigations

Table 5.5: Principal technical risks and mitigation actions.

Risk	Severity	Mitigation
Annulus too compliant after conductor cavities are added	High	include conductor packaging in first structural loop, not after CAD freeze
Segment joints become hot spots for current and stress	High	co-design the electrical window and structural insert; validate with coupon tests
Allocator excites structural modes under aggressive control action	Medium–High	include modal awareness and structural weighting in constrained allocation
Center-body interface becomes the dominant mass driver	High	treat it as a first-class work package and run early junction-load studies
Local battery fault propagates across one ring	High	use segmented isolation, decentralized modules, and explicit fault testing
Manufacturing complexity erodes modularity benefit	Medium	standardize segment lengths, inserts, and connector cartridges across the family

5.10 What constitutes success

At the end of the concept-maturation program, success should mean:

- the annulus structural section is frozen by correlated evidence,
- the IACC interconnect concept is demonstrated physically,
- a ring-aware allocator is operating on representative hardware,
- conductor mass and thermal behavior are quantified rather than guessed,
- the quad-ring 72/76 architecture has a defensible mass and power closure, and
- the program can choose rationally between semi-scale continuation, full-scale demonstrator work, or mission-specific derivative programs.

That is the threshold at which the ring-wing concept stops being merely intriguing and becomes a buildable aircraft architecture.

Chapter 6

Conclusions

The articulated ring-wing eVTOL family described in this white paper is structurally credible precisely because it is treated as a repeatable engineering primitive rather than as an artistic configuration. Each annulus bus is defined as a multi-function member that carries thrust loads, houses conductors, exposes modular interconnects, and participates in hierarchical control allocation. That definition turns the architecture into something that can be sized, modeled, built, and verified.

The main technical conclusions are straightforward:

- the 18/19-rotor annulus is a viable propulsion primitive for scaling into larger families;
- the quad-ring 72/76 configuration is the most natural next focus because it aligns with both the current repository logic and the existing 76-motor MATLAB reference;
- the annulus must be designed from the start as a conductor-bearing structural member, otherwise the modularity benefit is lost to harness complexity;
- control allocation should be ring-aware and should use excess actuator authority for structural load relief, thermal management, and degraded-mode resilience; and
- a disciplined concept-maturation program can substantiate the architecture with manageable cost and schedule if structural, electrical, and control work proceed as one integrated effort.

The package delivered here is intended to be the engineering starting point for that next step.

Appendix A

Rotor Coordinate Tables

A.1 One-ring normalized 19-rotor coordinates

Table A.1 lists the normalized coordinates generated for the 19-rotor annulus. These values are stored in `data/annulus_19_rotor_coordinates.csv` for direct reuse.

Table A.1: Normalized coordinates for the 19-rotor annulus. Outer-ring radius is normalized to 1.0 and the inner ring is set to 0.52.

Rotor ID	x/R_o	y/R_o
R00	0.0000	0.0000
R01	0.5200	0.0000
R02	0.2600	0.4503
R03	-0.2600	0.4503
R04	-0.5200	0.0000
R05	-0.2600	-0.4503
R06	0.2600	-0.4503
R07	0.9659	0.2588
R08	0.7071	0.7071
R09	0.2588	0.9659
R10	-0.2588	0.9659
R11	-0.7071	0.7071
R12	-0.9659	0.2588
R13	-0.9659	-0.2588
R14	-0.7071	-0.7071
R15	-0.2588	-0.9659
R16	0.2588	-0.9659
R17	0.7071	-0.7071

Rotor ID	x/R_o	y/R_o
R18	0.9659	-0.2588

A.2 MATLAB 76-motor reference inputs

The project already contains a 76-motor MATLAB model that repeats a 19-station quadrant pattern across four quadrants. Table A.2 reproduces the unique quadrant-arm data visible in `frameData76.m`; these values are useful as a cross-check when adapting the quad-ring configuration into a ring-native CAD layout.

Table A.2: Unique quadrant values excerpted from the workspace's 76-motor MATLAB file.

Station	Arm length [ft]	Arm angle [deg]
1	5.4	43.5
2	6.7	33.7
3	8.1	27.9
4	9.8	27.9
5	9.0	18.8
6	7.8	10.6
7	6.2	5.9
8	4.6	7.9
9	3.5	24.1
10	3.8	49.0
11	5.3	60.9
12	7.0	60.8
13	8.4	54.9
14	9.4	46.6
15	9.9	37.9
16	8.2	39.3
17	7.1	46.6
18	6.7	19.9
19	5.2	26.3

Appendix B

Code Listings

B.1 Mathematica annulus coordinate helper

Listing B.1: Core helper for generating evenly spaced points on a circle.

```
circleCoord[r_, numCircles_, thetaOffset_] :=
 Table[
   N[r*{Cos[theta + thetaOffset], Sin[theta + thetaOffset]}],
   {theta, 0, 2*Pi, (2*Pi)/numCircles}
 ][[;; -2]]
```

B.2 Ring-specific coordinate composition

Listing B.2: Suggested Mathematica composition for 18/19-rotor annulus coordinates.

```
outerRadius = 1.0;
innerRadius = 0.52 * outerRadius;
centerRotor = {{0., 0.}};
innerCoords = circleCoord[innerRadius, 6, 0];
outerCoords = circleCoord[outerRadius, 12, Pi/12];

coords19 = Join[centerRotor, innerCoords, outerCoords];
coords18 = Join[innerCoords, outerCoords];
```

B.3 Python figure-generation excerpt

Listing B.3: Excerpt from the delivered figure-generation script.

```python
def annulus_rotor_coordinates(
    outer_radius: float = 1.0,
    inner_radius_ratio: float = 0.52,
    include_center: bool = True,
) -> list[tuple[str, float, float]]:
    coords = []
    if include_center:
        coords.append(("R00", 0.0, 0.0))
    inner = circle_coord(outer_radius * inner_radius_ratio, 6, 0.0)
    outer = circle_coord(outer_radius, 12, math.pi / 12.0)
    for idx, (x, y) in enumerate(inner, start=1):
        coords.append((f"R{idx:02d}", x, y))
    for idx, (x, y) in enumerate(outer, start=7):
        coords.append((f"R{idx:02d}", x, y))
    return coords
```

B.4 MATLAB excerpt from the 76-motor frame reference

Listing B.4: Mass-property and projected-area excerpt from the workspace's MATLAB reference.

```matlab
MomentOfInertia(1) = sum(arm_weights .* arm_lengths_projected_on_yz .^ 2 / 3)
    ...
     + sum((motor_weight + propeller_weight) * (arm_lengths_projected_on_yz .^
        2));

MomentOfInertia(2) = sum(arm_weights .* arm_lengths_projected_on_xz .^ 2 / 3)
    ...
     + sum((motor_weight + propeller_weight) * (arm_lengths_projected_on_xz .^
        2));

MomentOfInertia(3) = sum(arm_weights .* arm_lengths .^2 / 3) ...
     + sum((motor_weight + propeller_weight) * (arm_lengths .^2));

projectedArea(3) = sum(arm_lengths * arm_width) ...
               + 1.22 * 0.76 ...
               + 0.508 * 0.0254 * 76;
```

Appendix C

Database and Parts-Selection Excerpts

C.1 Confirmed external repository values

After direct fetch of the referenced repository, the following sample entries were confirmed:

Table C.1: Sample parts entries confirmed in the cloned external repository.

Category	Part	Key data	Use in this white paper
Motor	4008 motor	87 g, 22.2 V, 17.15 A, 2496 g thrust	lightweight station sizing reference
Motor	5008 motor	138 g, 22.2 V, 33.3 A, 4072 g thrust	heavier station sizing reference
Battery	Tattu 6S 10000	1400 g, 22.2 V, 250 A, 10 000 mAh	development battery basis
Battery	Tattu 6S 20000	2540 g, 22.2 V, 250 A, 20 000 mAh	endurance trade studies
Battery	Tattu Plus 12S 22000	5800 g, 44.4 V, 550 A, 22 000 mAh	higher-voltage segmented-bus studies
PDB	PM07	43.8 g, 8 inputs, 90 A	ring-local distribution concept
PDB	300A top entry	110.9 g, 6 inputs, 300 A	center or segment interface concept

C.2 Example wire-length output

The 32-motor reference repo also contained a plain-text wire summary reporting approximately:

- 63 m red and 63 m black 16 AWG from fuselage to ESCs,
- 3 m each of three phase colors from ESCs to motors, and
- 23 m each for CAN ground, CAN-L, and CAN-H.

These values are included here because they illustrate how fast wiring quantities accumulate even before the aircraft reaches the ring counts addressed by this white paper.

Bibliography

[1] Aerial MECHANICA Inc. High-rotor count substantiation summary, 2026. Internal technical summary.

[2] AirGo Design Pte Ltd. Composite quadrant for v. arl-221111b, 2022. Internal structural report.

[3] AirGo Design Pte Ltd. Aerial industries structure concept v07 structure update 221006, 2022. Internal structure update memorandum.

[4] Minpei Chua. Parts selections and estimated weight calculations. https://github.com/minpei-chua/Parts-Selections-and-Estimated-Weight-Calculations, 2026. Repository containing motor, battery, PDB, and wire-routing datasets.

[5] European Union Aviation Safety Agency. Means of compliance with the special condition vtol (sc-vtol-3): Propulsion battery thermal runaway design and installation, 2023. URL https://www.easa.europa.eu/sites/default/files/dfu/MOC_SC-VTOL-3%20Issue%202.pdf.

[6] Arinze N. N. Eze, Kangni Combey, Federico N. Ramírez, and Sen Wang. Conceptual design of the urban air mobility common model multicopter aircraft, 2026. DICUAM 2026 conference paper.

[7] Arinze Ndubisi Eze. Articulated ring wing evtol structure with distributed propulsion and advanced dynamic payload stabilization system and integrated energy regeneration and safety systems, 2025. U.S. Patent Application No. 19/308,830 and related PCT filing.

[8] João Lima, Matheus Pereira, Sen Wang, Tze Lum, Tom Satendra, Sven Roelofsen, and Pieter Sijtsma. A preliminary design framework for performance and noise assessment of urban air mobility concepts. In *AIAA Aviation 2024 Forum*, 2024. AIAA 2024-3890.